

REVIEW ARTICLE

A polarizing situation: Taking an in-plane perspective for next-generation near-field studies

P. James Schuck^{1,†}, Wei Bao^{1,2}, Nicholas J. Borys¹

¹ Molecular Foundry, Lawrence Berkeley National Laboratory, Berkeley, CA 94720, USA

² Department of Materials Science and Engineering, University of California, Berkeley, CA 94720-1760, USA

Corresponding author. E-mail: [†]pjschuck@lbl.gov

Received September 15, 2015; accepted November 18, 2015

By enabling the probing of light–matter interactions at the functionally relevant length scales of most materials, near-field optical imaging and spectroscopy accesses information that is unobtainable with other methods. The advent of apertureless techniques, which exploit the ultralocalized and enhanced near-fields created by sharp metallic tips or plasmonic nanoparticles, has resulted in rapid adoption of near-field approaches for studying novel materials and phenomena, with spatial resolution approaching sub-molecular levels. However, these approaches are generally limited by the dominant out-of-plane polarization response of apertureless tips, restricting the exploration and discovery of many material properties. This has led to recent design and fabrication breakthroughs in near-field tips engineered specifically for enhancing in-plane interactions with near-field light components. This mini-review provides a perspective on recent progress and emerging directions aimed at utilizing and controlling in-plane optical polarization, highlighting key application spaces where in-plane near-field tip responses have enabled recent advancements in the understanding and development of new nanostructured materials and devices.

Keywords near-field optical microscopy, nano-optics, TERS, plasmonics, optical antenna, 2D materials

PACS numbers 78.67.-n, 78.67.Pt, 78.68.+m

Contents

- 1 Introduction
 - 2 Polarization properties of apertureless tips
 - 3 Measuring near-field tip polarizability
 - 4 Probing in-plane modes of nanomaterials
 - 4.1 Nano-mapping of in-plane vibrations in carbon nanotubes and graphene
 - 4.2 Hyperspectral nano-imaging of exciton properties in two-dimensional transition metal dichalcogenides
 - 5 Mapping nanoscale electric and magnetic vector fields
 - 6 Future directions and outlook
- Acknowledgements
References

1 Introduction

Near-field optical imaging and spectroscopy have undergone a renaissance of sorts, paralleling the past decade's enormous progress in nanoscale material design, structuring, synthesis, and control. The primary reasons for this are two-fold: (i) nano-optical approaches provide the opportunity to probe and control light–matter interactions and properties at the functionally relevant length scales of nanostructured materials; and (ii) the continued development of near-field probes has benefited greatly from recent advances in plasmonics, nanofabrication, and nanoassembly. Indeed, continually expanding near-field capabilities, combined with greatly reduced technical limitations, offer more access to physical and chemical information that is unobtainable with other methods.

At the core of all near-field studies is the near-field tip (also known as a near-field probe), which acts as a transducer for far- to near-field light and vice versa, ide-

*Special Topic: Frontiers of Plasmonics (Ed. Hong-Xing Xu).

ally providing an approximate optical “delta function” response (relative to a far-field diffraction-limited spot) at its apex [1–13]. More specifically, the tip modifies the local density of optical states within the zeptoliter mode volume surrounding its apex [1, 14–16]. Because it is responsible for mediating all nano-optical interactions with the sample, the quality and characteristics of all near-field images critically depend on the tip [17]. It can function either as a source of localized (near-field) light or as a reporter of the sample’s near-fields, and frequently acts as both. Either way, it is important to note that, upon optical excitation, the confined near fields surrounding both the sample and tip are highly complex. The fields have both electric (E) and magnetic (H) components consisting of a three-dimensional (3D) complex-valued polarization state (vector field) [18–21]. Notably, although near-fields are evanescent in nature, the concept of their degree of polarization can be well defined [22]. As a consequence, the tip’s interaction with a sample (and its ability to probe and influence local sample properties) is strongly dependent on its response to different electromagnetic field polarizations. *Thus, understanding and engineering the polarization response of near-field probes is crucial for unlocking the full potential of near-field microscopy, and ultimately for investigating and developing new materials and their properties.*

Indeed, knowledge and control of the probe’s polarization behavior is important for a wide range of applications. Besides the more-conventional polarimetry near-field scanning optical microscopy (NSOM) [23, 24], these include: full vector-field mapping of the nano-light surrounding next-generation nanophotonic devices [17]; mapping and controlling the radiative/nonradiative relaxation kinetics, dipole orientations and directional emission from nanoscale emitters [7, 25–38]; nanocrystallography investigations [39, 40]; and probing local nonlinear optical behavior [41–51] and magneto-optical effects [52–69]. Studies involving nanoscale vibrational spectroscopy and imaging are perhaps where the tip polarization response is most important, since a well-understood near-field polarization can reveal unique nanoscale properties such as molecular symmetry, intermolecular interactions, and bond orientations within a sample [40, 70–74]. This information is critical for developing technologies based on bio- and nanomaterials, where, for example, a tiny difference in molecular orientation can be of great functional importance [75]. In all cases, it is important to understand the polarization properties of the near-field tip for correctly interpreting the images or spectra that are recorded.

The original nano-aperture-based tip design enabled production of and interaction with near-fields that were

polarized predominantly in the plane of the sample surface (in-plane polarization) [Fig. 1(A)] [1, 9, 76–79]. However, the major signal-to-noise constraints and spatial resolution limitations of these tips (typically restricted to ~ 100 nm or larger) lead to *apertureless* NSOM approaches, in which the nanoscale aperture is replaced by (a much smaller) metallic particle [80] or a sharp metal-coated scan-probe tip [1]. Notably, the polarizability of these apertureless tips is principally in the out-of-plane or “z” direction [Fig. 1(B)] along the long-axis of the tip [1, 7, 40, 81]. Therefore, the advantages in resolution and signal enhancement afforded by apertureless tips, as well as the advances in commercially available instrumentation [82–84], mean that *a majority of recent near-field optical investigations have concentrated primarily on z-polarized interactions with samples*. While the tips are beneficial for probing a number of key interfacial properties (e.g. molecular adsorption), the exploration and discovery of many material properties (e.g. phonons and excitons in two-dimensional (2D) materials) requires interaction with in-plane near-field light components. This has led to recent design and fabrication breakthroughs in near-field tips engineered specifically for enhanced, higher-resolution in-plane interactions (see Fig. 1).

This mini-review provides a perspective on recent developments aimed at utilizing and controlling *in-plane* optical polarization within near-field studies of nanosstructured materials. The discussion will begin with a brief description of the polarization response of conventional apertureless near-field tips. We will then highlight key application spaces where in-plane near-field polarization studies have enabled recent advancements. Finally, we will discuss emerging prospects for controlling and converting between different near-field polarization states, as well as future directions directly impacted by better understanding, control, and enhancement of in-plane optical near-fields.

2 Polarization properties of apertureless tips

As noted above, sharp, metal near-field tips demonstrate a strongly anisotropic polarizability favoring the z-direction. This is clear for elongated or ellipsoidal tips oriented normal to the surface. However, even for a perfectly spherical metal nanoparticle at a tip apex, interactions with a sample (and broken symmetry along the axial direction) – with the tip/particle effectively coupling with an image dipole beneath the sample surface [Fig. 1(B)] – lead to preferential polarizability, local field enhancement, and scattering for z-polarized fields [4]. A phenomenological model has been successfully employed

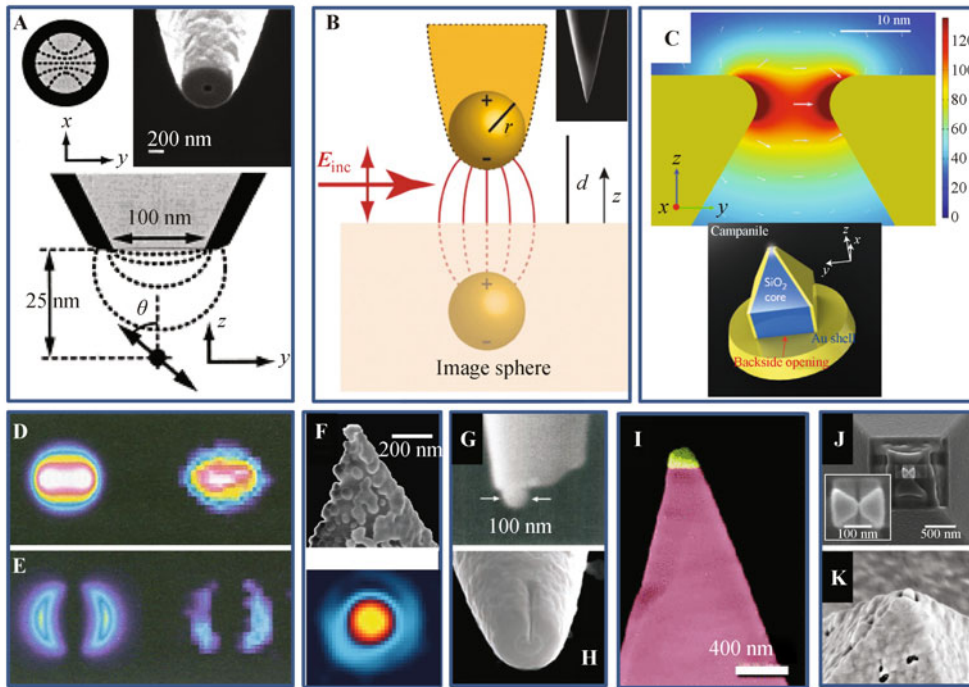


Fig. 1 Examples of NSOM tips with different electromagnetic field polarization responses. **(A)** Schematic of an aperture-based NSOM tip as seen from below (upper left) and as a section along the tip axis (bottom), as well as its associated electric field lines (dotted). Adapted from Ref. [116]. Inset: scanning electron microscope (SEM) image of an aluminum-coated aperture-based NSOM tip. Reproduced from Ref. [34]. **(B)** Model of an apertureless tip and the effective polarizability of this coupled tip-sample system approximating the tip as a sphere with radius r and tip-sample separation d and subject to an external field \mathbf{E}_{inc} . Reproduced from Ref. [4]. Inset: SEM Image of a sharp metal apertureless tip courtesy of Lukas Novotny. Used with permission (www.nano-optics.org). **(C)** A yz -section simulation of the spatial profile of the steady state electric field amplitude near the end of a Campanile tip, normalized to the incident field amplitude (top). The white arrows indicate the polarization of the electric field. A schematic of a Campanile structure at the end of a gold-coated conical tapered NSOM fiber (bottom). Adapted from Ref. [191]. **(D)** Simulated $|E_x|^2$ distribution near an aperture NSOM tip (left) and the measured image of an in-plane oriented fluorescent molecule (right). **(E)** Similar to (D), but for the $|E_z|^2$ component distribution (left) and an out-of-plane oriented molecule (right); all for x -polarized tip excitation. (E) and (D) adapted from Ref. [26]. **(F)** SEM image of a granular metallic tip made by evaporating Ag on a silicon cantilever for AFM (top) and the experimental defocused scattering pattern from the same tip (bottom) illustrating its dipole orientation. Reproduced from Ref. [71]. **(G)** SEM image of a Au nanosphere at the end of a glass fiber tip. Reproduced from Ref. [80]. **(H)** SEM image of a split-ring aperture probe for measuring optical magnetic fields. Reproduced from Ref. [222]. **(I)** SEM image of a triangular Pt antenna probe fabricated on a Si AFM tip, with Pt highlighted in yellow and Si in red. Reproduced from Ref. [200]. **(J)** SEM image of a bowtie nanoantenna tip. Reproduced from Ref. [30]. **(K)** SEM image of a coaxial nanoantenna tip. Reproduced from Ref. [84].

to describe the polarization-selective enhancement of apertureless tips, especially in the context of references [39, 85, 86]. Here, the Raman scattering tensor \mathbf{R} , which describes the far-field polarization selection rules for Raman scattering, is modified by “tip-amplification tensors” \mathbf{F} and \mathbf{F}' to account for the polarization-selective enhancement of the excitation and subsequent scattering into the far-field, respectively. In the presence of a tip, the tip-enhanced Raman scattering (TERS) tensor becomes: $\mathbf{R}_{\text{TERS}} = \mathbf{F}^T \mathbf{R} \mathbf{F}'$. The values of the tip-amplification tensors depend on the exact geometry of the tip in a manner similar to its polarizability [48], and they are typically assumed to have the form:

$$\mathbf{F}(\omega) = \begin{pmatrix} F_x & 0 & 0 \\ 0 & F_y & 0 \\ 0 & 0 & F_z \end{pmatrix},$$

$$\mathbf{F}' = \mathbf{F}(\omega') = \begin{pmatrix} F'_x & 0 & 0 \\ 0 & F'_y & 0 \\ 0 & 0 & F'_z \end{pmatrix}$$

where $F_z > F_x$, $F_y > F'_x$, $F'_y > F'_z$. Here, ω and ω' are the incident optical frequency and scattered output signal frequency, respectively. Often, the frequency difference $\omega - \omega'$ can be small relative to the plasmon resonance width of the tip, such that $\mathbf{F} \cong \mathbf{F}'$.

Such tip-enhancement tensors well describe the polarization selectivity that can be achieved with an apertureless probe with the assumption that the off-diagonal elements equal 0, which is proving adequate for many applications. z -polarized apertureless near-fields have proven to be powerful, e.g., for Raman-based nanocrystallography studies [39], TERS measurements of

compositional and strain gradients [42, 74, 87–104], nano-IR spectroscopic imaging of proteins and other soft materials [105–111], and fluorescence mapping of oriented molecules [25, 28, 31–33, 112–117]. The sensitivity is further enhanced by using second harmonic generation and other nonlinear optical contrast mechanisms for probing broken symmetries in materials (e.g. ferromagnetic domains) at the nanoscale [44, 46, 47, 67, 118]. Importantly, in nearly all these cases, contributions from the more weakly enhanced *x, y-polarization in: x, y-polarization out* configuration are neglected.

However, many critical electronic and vibrational excitations – particularly in lower-dimensional nanomaterials – are sensitive only to in-plane field polarizations. Additionally, detailed light–matter interactions within the tip’s near-field can be considerably more complex than those described by the above tensors. For example, in Figs. 1(A–C), note that the polarization is “pure” (either completely in-plane or out-of-plane) only directly along the tip axis [Fig. 1(B)] or in the center of the aperture or gap [Fig. 1(A,C)], whereas all other locations experience depolarization (i.e., the off-diagonal elements in \mathbf{F} , \mathbf{F}' are not 0). Further polarization mixing results from a tip’s finite cone or pyramid angles, tip tilt, and nanoscale tip inhomogeneities [86, 119, 120]. Phenomenological models can capture the cross-polarization effects of cone/pyramid angles and tip tilt quite well, and it has even been shown that a higher signal contrast in TERS experiments is possible under cross-polarized detection (*z* polarized excitation, in-plane detection) [86, 119].

3 Measuring near-field tip polarizability

Nearly all near-field tips exhibit some degree of structural heterogeneity at the nanoscale, adding variability to their near-field properties. Thus, while theoretical simulations – both analytical and numerical – can qualitatively describe the polarization response of model near-field tips, the desire for a more quantitative understanding of this has led to the development of techniques for performing near-field polarization analysis on real probes. This is particularly relevant for some recent tip designs, where a degree of intentional heterogeneity, or “controlled roughness”, is exploited for improved light capture and enhancement properties in TERS measurements [Fig. 1(F)] [71].

From the 1990s, researchers were able to use single molecules as probes to determine the orientation of near-fields [e.g. Figs. 1(D, E)] [26, 121, 122]. However, despite providing extremely high-resolution spatial information,

single-molecule near-field fluorescence measurements are not particularly high throughput ones; hence other tip-characterization approaches were developed. For example, in 2007, Lee *et al.* showed that a conventional ellipsometry method, the so-called rotational analyzer ellipsometry technique, was capable of determining the polarizability tensor of Au-nanoparticle-functionalized tips [Fig. 1(G)] [123]. In this method, the tensor is built up serially by systematically rotating the polarizer angle in the scattered-light detection path for all incident light polarizations. More recently, Mino *et al.* showed that a defocused imaging approach could be used for establishing the tip apex polarizability based on a single measured scattering pattern [Fig. 1(F)] [71]. Others have employed back focal plane imaging to measure the dipole orientation of metal nanoparticles [124] and other structures [125–130]. Compared to defocused imaging, back focal plane imaging is advantageous when the tip polarization/dipole is primarily in-plane. However, defocused imaging is better for probing *z*-oriented dipoles and is less sensitive to laser speckle noise from Raleigh scattered light. In all cases, it was established that once the tip polarizability is determined, it becomes possible to *quantitatively* interpret near-field TERS [71] and vector-field maps [19, 123] obtained with the same tips – a key goal of near-field microscopy.

4 Probing in-plane modes of nanomaterials

As mentioned above, some classes of polarization-sensitive measurements such as single-molecule fluorescence and magneto-optical studies are amenable to the use of conventional aperture-based NSOM probes and thus, their in-plane polarization response. However, many other spectroscopy methods, particularly chemical imaging via vibrational spectroscopy, require signal enhancement that is achievable only with apertureless and other more-advanced tips.

4.1 Nano-mapping of in-plane vibrations in carbon nanotubes and graphene

Carbon nanotubes (CNTs), along with being considered a fundamental “nano building block” for many potential technologies [131], are a prototypical nanomaterial whose spectroscopic properties require probing with in-plane polarization components [Figs. 2(A–F)] [71, 74, 132]. In particular, the G+ Raman band at $\sim 1580 \text{ cm}^{-1}$ [Figs. 2(B, C)], a longitudinal optical phonon related to C-C bond stretching, is most sensitive to polarization along the tube axis. The Raman spectra of this and other re-

lated G modes can indicate external stresses acting on a CNT and provide information on CNT chirality. Meanwhile, the radial breathing mode (RBM) [Fig. 2(B, D)], with energies in the $\sim 100\text{--}400\text{ cm}^{-1}$ range, responds primarily to z -polarized field components and provides a direct measure of the CNT diameter. Additional Raman modes include the disorder-induced D band at $\sim 1300\text{ cm}^{-1}$, as well as the in-plane-sensitive Z-breathing modes [133] along the CNT axis with low and intermediate energies corresponding to the lengths of short tubes or tube segments [Fig. 2(B)] [134–141]. In fact, with such well-defined modes, CNTs are excellent test beds for under-

standing in- vs. out-of-plane near-field tip polarization properties [71].

Near-field capabilities have proven invaluable for CNT characterization, enabling numerous nanoscale insights into local CNT physics, structure, and behavior [Figs. 2(A, E, F)]. For example, TERS and nanophotoluminescence (nano-PL) measurements have revealed local distortions of the CNT lattice by a negatively charged defect [142], as well as local changes in chirality and conductivity [143]. However, the weaker in-plane polarizability and field enhancement capabilities of conventional apertureless probes, combined with larger

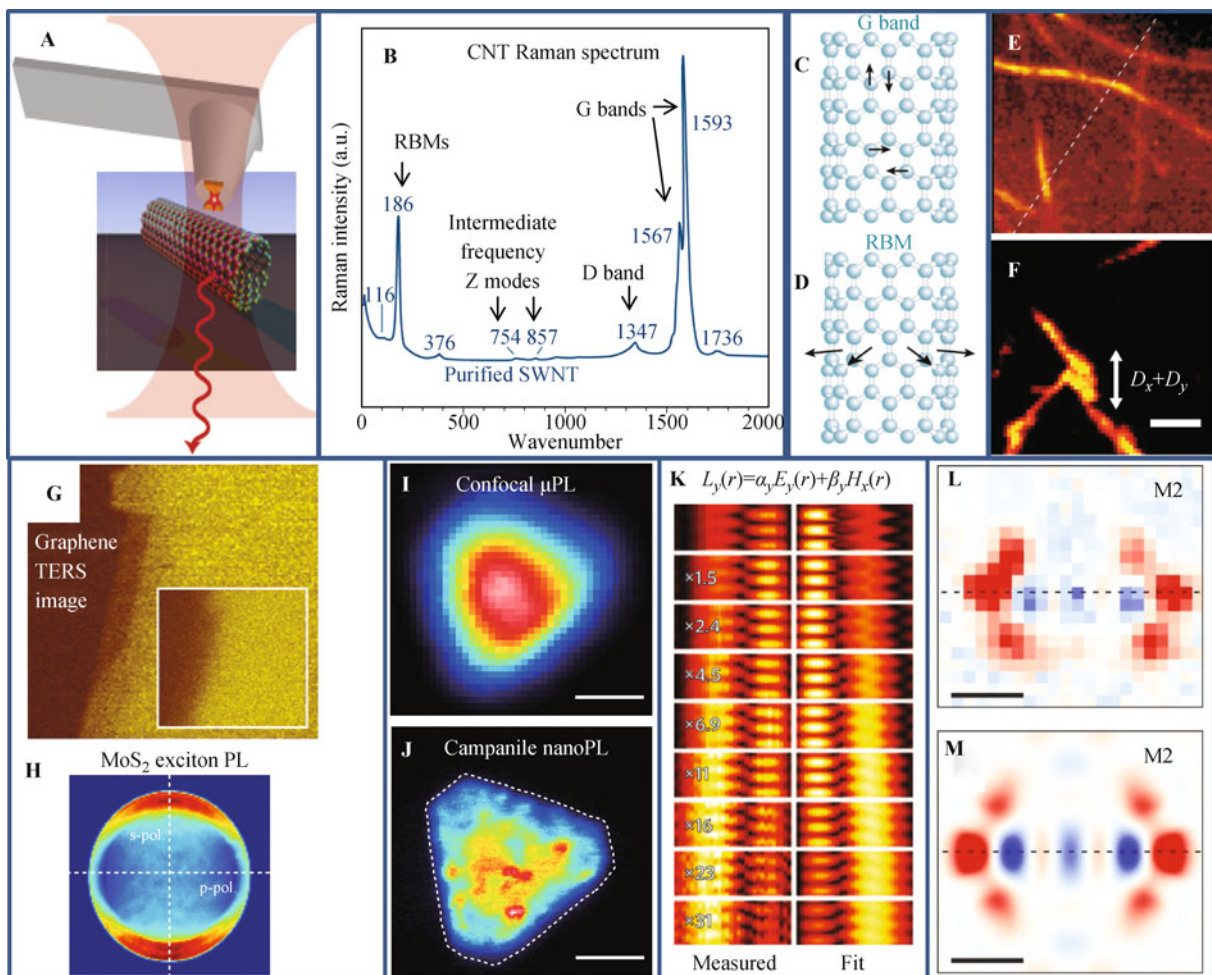


Fig. 2 Applications of polarization-dependent NSOM. (A) Schematic of a TERS measurement on a CNT using a bowtie nanoantenna tip with in-plane polarizability. Adapted from Ref. [6]. (B) A representative Raman spectrum from a single-wall CNT bundle. (C) The G-band eigenvectors for the CNT C-C bond stretching mode. (D) CNT radial breathing mode eigenvectors. (B–D) figures and captions adapted from Ref. [132]. (E) Apertureless TERS image of single-wall CNTs. Reproduced from Ref. [104]. (F) TERS image of single-wall CNTs taken with tip similar to that shown in Fig. 1(F). The white arrow shows the in-plane components of the tip dipole, $D_x + D_y$. Reproduced from Ref. [71]. (G) Graphene TERS image of the G' band. Inset: confocal image of the same area. Adapted from Ref. [146]. (H) Back focal plane emission pattern from a MoS_2 monolayer showing purely in-plane exciton dipole emission. Adapted from Ref. [186]. (I) Confocal micro-PL image and (J) Campanile near-field nano-PL image of the same monolayer MoS_2 flake. Adapted from Ref. [193]. (K) Aperture-based NSOM measurements, and fits, at different heights above a photonic crystal waveguide containing information of both in-plane optical electric and magnetic fields. Adapted from Refs. [17] and [231]. (L) Measured and (M) calculated electric (red) and magnetic (blue) field intensity distributions above a photonic crystal nanocavity. The measured fields were collected with a Campanile tip. Reproduced from Ref. [232].

background signals, have limited the extension of these types of near-field optical characterization techniques to graphene [102, 144–147] (though nano-IR measurements have proven invaluable for probing plasmons in graphene and CNTs [148–154]). The phonon properties of graphitic films are dominated by the planar symmetry of the material, making the G phonons relatively inaccessible to the conventional TERS response [145]. Still, broken symmetries, defects, and edges can result in stronger out-of-plane TERS coupling and hence have recently resulted in some exciting investigations of nanoscale graphene properties [Fig. 2(G)] [145, 146].

The clear advantages of in-plane polarized near-fields for CNT (and graphene) TERS studies have motivated the use of more sophisticated probes [5, 6, 155, 156] based on optical nanoantennas [157–160]. Such probes include bowtie-antenna tips [e.g. Fig. 1(J) and Fig. 2(A)] [6, 30, 161, 162] and resonant coaxial antenna tips [e.g. Fig. 1(K)] [84, 163]. In CNT studies, these tips demonstrated both significant in-plane TERS signal enhancement while using dielectric substrates (previous enhancements of similar magnitude were achieved only with metal tips over metal substrates in the so-called tip-substrate gap mode) [6] and the ability to probe the Z-breathing intermediate-frequency Raman modes, which are typically very weak or absent in conventional Raman spectroscopy of CNTs [133].

4.2 Hyperspectral nano-imaging of exciton properties in two-dimensional transition metal dichalcogenides

Due to their remarkable light absorption and emission properties – and the unparalleled opportunities for dynamically controlling them – 2D monolayer transition metal dichalcogenides (ML-TMDCs) are ideal building blocks for atomically thin, flexible optoelectronic devices [164–176]. They exhibit unique properties and physics not seen in other 2D materials; for example, unlike graphene, many members of the TMDC family have appreciable direct bandgaps, typically in the ~1–3 eV range [175–178]. They are therefore genuine semiconductors that interact strongly with near-infrared and visible light (e.g., a monolayer of MoS₂ absorbs up to ~30% of incident light with above-gap energies), making them particularly appealing for a plethora of light absorbing and/or emitting device applications [165, 172, 179–181]. The near-band-edge optical transitions in ML-TMDCs are dominated by excitons and trions (charged excitons) [182]. And unlike traditional 2D quantum wells, the enhanced coulombic interaction between the electrons and holes in ML-TMDCs stabilizes the excitonic states at room temperature with exceptionally large binding en-

ergies (~0.5–1 eV) [177, 178, 183, 184].

Unfortunately, the performance of the active ML-TMDC materials is often far below theoretical expectations, particularly for critical factors such as carrier mobility and quantum yield [165, 185]. This can be traced to a few key factors, with the primary one being a notable lack of nanoscale characterization studies, especially ones pertaining to optical properties; to date, nearly all optical investigations of ML-TMDCs have been diffraction-limited. This is related to the fact that the primary excited state absorbers/emitters in these systems – excitons – are polarized *within the plane of the 2D layer* [186], making them less sensitive to conventional apertureless tip near-field characterization approaches. This, combined with larger background signal issues inherent in 2D material studies, means near-field studies on ML-TMDCs and related materials have been successfully realized only recently [187–190, 193].

These investigations are enabled by next-generation near-field probes engineered for in-plane polarizability. The Campanile tip geometry [Fig. 1(C)] has proven particularly useful [191, 192], recently facilitating hyperspectral mapping of nanoscale excited state relaxation processes in MoS₂ [Figs. 2(I, J)] [193]. These nano-optical studies succeeded in determining and visualizing optoelectronic and excitonic properties, heterogeneity, and band-bending at the most relevant and important length scales in these materials. The (mesoscopic) effects of grain boundaries on these properties were directly imaged and quantified, with significant implications for device design. Most notably, near-field probing led to the discovery of a surprising new form/phase of MoS₂ at the edge region of all synthetic/CVDchemical vapor deposition-grown materials. This is particularly important, as it constitutes a paradigm shift from only metallic states in the interpretation of edge-related physics and photochemistry in synthetic 2D materials, and has a profound impact on both catalytic applications and device technologies, as it is a critical consideration for establishing electrical contact [194].

These studies represent only the beginning of (in-plane polarized) near-field efforts aimed at elucidating the rich and unique nanoscale physics within these exciting 2D systems, ultimately guiding the future development of high-quality layered materials and next-generation devices that are expected to impact an incredibly broad range of applications.

5 Mapping nanoscale electric and magnetic vector fields

Lower-dimensional material systems, such as those de-

scribed above, often act as the basic building blocks for novel nanophotonic device structures that are designed to control and transform light at deeply subwavelength scales. Owing to the needs of an ever-expanding application space that requires finer nano-optical control and expanded functionalities, it is critical to map the complex EM fields surrounding these device elements for characterizing, understanding, and engineering their nano-light properties. As highlighted in a recent review [17], great strides in this area of nano-optical characterization now allow researchers to probe different phase and amplitude vector components of both electric and magnetic fields at the nanoscale. Needless to say, the in-plane as well as out-of-plane field components should be effectively measured for obtaining a complete picture of how these nanophotonic elements interact and ultimately perform together.

Over the past 10 years, researchers have shown that standard apertureless tips can successfully map the x , y and z components of the electric field vector \mathbf{E} (and even magnetic field intensities [195]) of a multitude of nanophotonic structures including plasmonic nanoparticles and cubes, optical antennas, split-ring resonators, and meta molecules [18–20, 123, 196–211]. Similarly, a well-characterized nanoparticle was recently used to visualize vector light-field distributions of tightly focused vector beams [212]. These experiments exploit the interference-based amplification techniques employed in scattering-type scanning near-field microscopy to measure both the field's amplitude and phase at each point in the scan [213], albeit with a much larger response to the z component, as noted above. Realizing the need for better in-plane sensitivity, Olmon *et al.* developed a probe consisting of a triangular Pt platelet oriented under a slight tilt angle at the tip apex, demonstrating good in- and out-of-plane response, as well as minimal depolarization effects [Fig. 1(I)] [200]. They used this probe to sensitively map the 3D vector electric near-field distribution surrounding an IR dimer optical antenna, and then take advantage of vector relationships to deduce the structure's conduction current density distribution \mathbf{J} and its associated magnetic vector field \mathbf{H} .

Aperture-based probes have proven to be quite adept at visualizing in-plane-polarized complex vector electric near-fields with high resolution using interferometric techniques [214, 215] to measure the amplitude and phase of \mathbf{E} surrounding structures such as plasmonic nanowires, negative index metamaterials, nanoapertures, dielectric-clad waveguides and photonic crystal waveguides [216–221]. Of course, mapping the local \mathbf{E} is just half the story, since novel materials (metamaterials) and nanostructures can have magnetic responses on par with electric responses, and also because local

charges and currents create \mathbf{E} and \mathbf{H} fields that are neither orthogonal nor equal in strength, leading to a nontrivial relationship between them. Researchers realized that an aperture probe can detect the z -component of the optical magnetic field, H_z , near photonic structures (either by using a modified “split-ring” aperture tip [222] [Fig. 1(H)] or through an H_z -mediated interaction with localized EM fields [223–226]) and also act as a Bethe-hole analyzer capable of sensing in-plane optical magnetic fields [227–230]. This has enabled simultaneous mapping of the amplitude and phase of \mathbf{E} and \mathbf{H} fields, as demonstrated by le Feber *et al.*, for the near-fields of a photonic crystal waveguide [Fig. 2(K)] [231]. Pushing the limits of sensitivity and resolution even further, researchers have recently shown that the Campanile near-field probes – with their stronger field confinement and larger field enhancement than aperture probes – can simultaneously measure in-plane E and out-of-plane H near-fields [Figs. 2(L, M)] [232]. Though the origins of the H -field responses for these various tips are still being clarified [17, 231–233], it is clear that a near-complete mapping of near-field vectors is now possible, representing a significant advance in nano-optical device characterization capabilities.

6 Future directions and outlook

Clearly, exciting and interacting with in-plane optical near-field polarization components is required to fully access nanostructured material properties at their most relevant length scales. To this end, current advances in near-field probe and nanoantenna development with significant in-plane polarizabilities and ultra-enhanced, strongly localized fields are central to a number of emerging nano-optical applications. For example, while the first calculations on optical trapping at the apex of an apertureless probe [234] have not resulted in a convincing demonstration, in-plane plasmonic aperture-antenna tips are now enabling trapping, spectroscopic interrogation, and manipulation of truly nanoscale objects [235–238] down to the size of individual proteins [239, 240]. The local gradient and scattering forces between a sharp tip's near-field and a photo-excited sample are now being exploited as a readout mechanism for a material's local chemistry and polarization [241–245]. Nonlinear vibrational nano-spectroscopies such as tip-enhanced stimulated Raman scattering [241] can now be employed to map in-plane vibrations and bond orientations (to date, only out-of-plane contributions have been probed [99]), further enhancing their chemical contrast capabilities, potentially down to the single-bond

level. On-demand catalysis with molecular precision can be enabled by polarization-sensitive plasmon-enhanced hot-carrier extraction [246–249]. When integrated into a heat-assisted magnetic recording scheme [250, 251], polarization-selective tips have been proposed as potential technologies for all-optical high-density memory read-write heads exploiting nanoscale magneto-optical interactions [252, 253]. Meanwhile, tips based on antennas that interact strongly with multiple E polarization components simultaneously [160, 254–256] would be capable of directly converting these components to circularly/elliptically polarized and even super-chiral near-fields [257–260], enabling unprecedented interactions with (chiral) nano-objects ranging from biomolecules to circular excitonic emitters within 2D TMDCs [179]. Indeed, modified next-generation probes are well-suited to act as nanophotonic-structured waveguides that efficiently collect and direct polarization-dependent emission from such excitonic photon sources, a function important for future solid-state quantum architectures [261, 262]. Of course, a number of near-field-related questions also exist, such as how can one perform near-field chemical imaging on a cell membrane or other soft material within a liquid? Can polarization at a tip apex ever be “pure” enough to sensitively measure Kerr rotations and related phenomena? Some exciting recent near-field time-resolved Kerr experiments suggest so [263], though it remains to be seen if this can be pushed from a ~ 100 nm resolution level to below 10 nm. Despite these and other challenges, it is evident that nearly all areas of science and technology stand to benefit from the pursuit of complete near-field polarization control.

Acknowledgements The authors thank our colleagues at the Molecular Foundry for stimulating discussion and assistance. Work at the Molecular Foundry was supported by the Director, Office of Science, Office of Basic Energy Sciences, Division of Materials Sciences and Engineering, of the U.S. Department of Energy under Contract No. DE-AC02-05CH11231.

Open Access The articles published in this journal are distributed under the terms of the Creative Commons Attribution 4.0 International License (<http://creativecommons.org/licenses/by/4.0/>), which permits unrestricted use, distribution, and reproduction in any medium, provided you give appropriate credit to the original author(s) and the source, provide a link to the Creative Commons license, and indicate if changes were made.

References

1. L. Novotny and B. Hecht, *Principles of Nano-Optics*, Cambridge: Cambridge University Press, 2006
2. S. Kawata, Y. Inouye, and P. Verma, Plasmonics for near-field nano-imaging and superlensing, *Nat. Photonics* 3(7), 388 (2009)
3. M. A. Paesler and P. J. Moyer, *Near-Field Optics: Theory, Instrumentation and Applications*, New York: Wiley, 1996
4. J. M. Atkin, S. Berweger, A. C. Jones, and M. B. Raschke, Nano-optical imaging and spectroscopy of order, phases, and domains in complex solids, *Adv. Phys.* 61(6), 745 (2012)
5. M. Fleischer, Near-field scanning optical microscopy nanoprobes, *Nanotechnology Reviews* 1(4), 313 (2012)
6. P. J. Schuck, A. Weber-Bargioni, P. D. Ashby, D. F. Ogle-tree, A. Schwartzberg, and S. Cabrini, Life beyond diffraction: Opening new routes to materials characterization with next-generation optical near-field approaches, *Adv. Funct. Mater.* 23(20), 2539 (2013)
7. N. Mauser and A. Hartschuh, Tip-enhanced near-field optical microscopy, *Chem. Soc. Rev.* 43(4), 1248 (2014)
8. A. V. Zayats and D. Richards (Eds.), *Nano-Optics and Near-Field Optical Microscopy*, Artech House, 2008
9. R. C. Dunn, Near-field scanning optical microscopy, *Chem. Rev.* 99(10), 2891 (1999)
10. M. I. Stockman, Nanoplasmonics: The physics behind the applications, *Phys. Today* 64(2), 39 (2011)
11. A. Hartschuh, Tip-enhanced near-field optical microscopy, *Angew. Chem. Int. Ed.* 47(43), 8178 (2008)
12. B. S. Yeo, J. Stadler, T. Schmid, R. Zenobi, and W. H. Zhang, Tip-enhanced Raman spectroscopy – Its status, challenges and future directions, *Chem. Phys. Lett.* 472(1–3), 1 (2009)
13. B. Pettinger, P. Schambach, C. J. Villagomez, and N. Scott, Tip-enhanced Raman spectroscopy: Near-fields acting on a few molecules, in: *Annual Review of Physical Chemistry*, M. A. Johnson and T. J. Martinez (Eds.), 2012, pp 379–399
14. K. Joulain, R. Carminati, J. P. Mulet, and J. J. Greffet, Definition and measurement of the local density of electromagnetic states close to an interface, *Phys. Rev. B* 68(24), 245405 (2003)
15. R. Beams, D. Smith, T. W. Johnson, S. H. Oh, L. Novotny, and A. N. Vamivakas, Nanoscale fluorescence lifetime imaging of an optical antenna with a single diamond NV center, *Nano Lett.* 13(8), 3807 (2013)
16. R. Carminati, A. Caze, D. Cao, F. Peragut, V. Krachmalnicoff, R. Pierrat, and Y. De Wilde, Electromagnetic density of states in complex plasmonic systems, *Surf. Sci. Rep.* 70(1), 1 (2015)
17. N. Rotenberg and L. Kuipers, Mapping nanoscale light fields, *Nat. Photonics* 8(12), 919 (2014)
18. M. Schnell, A. Garcia-Etxarri, J. Alkorta, J. Aizpurua, and R. Hillenbrand, Phase-resolved mapping of the near-field vector and polarization state in nanoscale antenna gaps, *Nano Lett.* 10(9), 3524 (2010)
19. K. G. Lee, H. W. Kihm, J. E. Kihm, W. J. Choi, H. Kim, C. Ropers, D. J. Park, Y. C. Yoon, S. B. Choi, H. Woo, J. Kim, B. Lee, Q. H. Park, C. Lienau, and D. S. Kim, Vector field microscopic imaging of light, *Nat. Photonics* 1(1), 53 (2007)

20. H. Gersen, L. Novotny, L. Kuipers, and N. F. van Hulst, On the concept of imaging nanoscale vector fields, *Nat. Photonics* 1(5), 242 (2007)
21. M. Born and E. Wolf, Principles of Optics: Electromagnetic Theory of Propagation, Interference and Diffraction of Light, 7th Ed., Cambridge: Cambridge University Press, 1999
22. T. Setala, A. Shevchenko, M. Kaivola, and A. T. Friberg, Degree of polarization for optical near fields, *Phys. Rev. E* 66(1), 016615 (2002)
23. S. Patanè, E. Cefali, S. Spadaro, R. Gardelli, M. Albani, and M. Allegrini, Polarization-maintaining near-field optical probes, *Journal of Microscopy* 229(2), 377 (2008)
24. M. J. Fasolka, L. S. Goldner, J. Hwang, A. M. Urbas, P. Derege, T. Swager, and E. L. Thomas, Measuring local optical properties: Near-field polarimetry of photonic block copolymer morphology, *Phys. Rev. Lett.* 90(1), 016107, 1 (2003)
25. P. Anger, P. Bharadwaj, and L. Novotny, Enhancement and quenching of single-molecule fluorescence, *Phys. Rev. Lett.* 96(11), 113002 (2006)
26. E. Betzig and R. J. Chichester, Single molecules observed by near-field scanning optical microscopy, *Science* 262(5138), 1422 (1993)
27. H. Eghlidi, K. G. Lee, X. W. Chen, S. Gotzinger, and V. Sandoghdar, Resolution and enhancement in nanoantenna-based fluorescence microscopy, *Nano Lett.* 9(12), 4007 (2009)
28. S. Kühn, U. Häkanson, L. Rogobete, and V. Sandoghdar, Enhancement of single-molecule fluorescence using a gold nanoparticle as an optical nanoantenna, *Phys. Rev. Lett.* 97(1), 017402 (2006)
29. P. Bharadwaj, P. Anger, and L. Novotny, Nanoplasmonic enhancement of single-molecule fluorescence, *Nanotechnology* 18(4), 044017 (2007)
30. J. N. Farahani, D. W. Pohl, H. J. Eisler, and B. Hecht, Single quantum dot coupled to a scanning optical antenna: A tunable superemitter, *Phys. Rev. Lett.* 95(1), 017402 (2005)
31. J. M. Gerton, L. A. Wade, G. A. Lessard, Z. Ma, and S. R. Quake, Tip-enhanced fluorescence microscopy at 10 nanometer resolution, *Phys. Rev. Lett.* 93(18), 180801 (2004)
32. A. Ghimire, E. Shafran, and J. M. Gerton, Using a sharp metal tip to control the polarization and direction of emission from a quantum dot, *Sci. Rep.* 4, 6456 (2014)
33. T. H. Taminiau, R. J. Moerland, F. B. Segerink, L. Kuipers, and N. F. van Hulst, $\lambda/4$ resonance of an optical monopole antenna probed by single molecule fluorescence, *Nano Lett.* 7(1), 28 (2007)
34. J. A. Veerman, A. M. Otter, L. Kuipers, and N. F. van Hulst, High definition aperture probes for near-field optical microscopy fabricated by focused ion beam milling, *Appl. Phys. Lett.* 72(24), 3115 (1998)
35. R. Eckel, V. Walhorn, C. Pelargus, J. Martini, J. Enderlein, T. Nann, D. Anselmetti, and R. Ros, Fluorescence-emission control of single CdSe nanocrystals using gold-modified AFM tips, *Small* 3(1), 44 (2007)
36. E. Yoskovitz, D. Oron, I. Shweky, and U. Banin, Apertureless near-field distance-dependent lifetime imaging and spectroscopy of semiconductor nanocrystals, *J. Phys. Chem. C* 112(42), 16306 (2008)
37. V. V. Protasenko, M. Kuno, A. Gallagher, and D. J. Nesbitt, Fluorescence of single ZnS overcoated CdSe quantum dots studied by apertureless near-field scanning optical microscopy, *Opt. Commun.* 210(1–2), 11 (2002)
38. M. I. Stockman, D. J. Bergman, and T. Kobayashi, Coherent control of nanoscale localization of ultrafast optical excitation in nanosystems, *Phys. Rev. B* 69(5), 054202 (2004)
39. S. Berweger, C. C. Neacsu, Y. B. Mao, H. J. Zhou, S. S. Wong, and M. B. Raschke, Optical nanocrystallography with tip-enhanced phonon Raman spectroscopy, *Nat. Nanotechnol.* 4(8), 496 (2009)
40. S. Berweger, J. M. Atkin, R. L. Olmon, and M. B. Raschke, Light on the tip of a needle: Plasmonic nanofocusing for spectroscopy on the nanoscale, *J. Phys. Chem. Lett.* 3(7), 945 (2012)
41. E. J. Sánchez, L. Novotny, and X. S. Xie, Near-field fluorescence microscopy based on two-photon excitation with metal tips, *Phys. Rev. Lett.* 82(20), 4014 (1999)
42. T. Ichimura, N. Hayazawa, M. Hashimoto, Y. Inouye, and S. Kawata, Tip-enhanced coherent anti-Stokes Raman scattering for vibrational nanoimaging, *Phys. Rev. Lett.* 92(22), 220801 (2004)
43. S. Palomba and L. Novotny, Near-field imaging with a localized nonlinear light source, *Nano Lett.* 9(11), 3801 (2009)
44. A. V. Zayats and V. Sandoghdar, Apertureless scanning near-field second-harmonic microscopy, *Opt. Commun.* 178(1–3), 245 (2000)
45. A. V. Zayats and V. Sandoghdar, Apertureless near-field optical microscopy via local second-harmonic generation, *Journal of Microscopy* 202(1), 94 (2001)
46. A. V. Zayats and I. I. Smolyaninov, Near-field second-harmonic generation: One contribution of 13 to a Theme “Nano-optics and near-field microscopy”, *Royal Society of London Transactions Series A*, 362(1817), 843 (2004)
47. C. C. Neacsu, B. B. van Aken, M. Fiebig, and M. B. Raschke, Second-harmonic near-field imaging of ferroelectric domain structure of YMnO₃, *Phys. Rev. B* 79(10), 100107 (2009)
48. C. Neacsu, G. Steudle, and M. Raschke, Plasmonic light scattering from nanoscopic metal tips, *Appl. Phys. B* 80(3), 295 (2005)
49. K. A. Meyer, K. C. Ng, Z. Gu, Z. Pan, W. B. Whitten, and R. W. Shaw, Combined apertureless near-field optical second-harmonic generation/atomic force microscopy imaging and nanoscale limit of detection, *Appl. Spectrosc.* 64(1), 1 (2010)
50. S. I. Bozhevolnyi, K. Pedersen, T. Skettrup, X. S. Zhang, and M. Belmonte, Far- and near-field second-harmonic imag-

- ing of ferroelectric domain walls, *Opt. Commun.* 152(4–6), 221 (1998)
51. L. Mahieu-Willame, S. Gresillon, M. Cuniot-Ponsard, and C. Boccara, Second harmonic generation in the near field and far field: A sensitive tool to probe crystalline homogeneity, *J. Appl. Phys.* 101(8), 083111 (2007)
 52. E. Betzig, P. L. Finn, and J. S. Weiner, Combined shear force and near-field scanning optical microscopy, *Appl. Phys. Lett.* 60(20), 2484 (1992)
 53. E. Betzig and J. K. Trautman, Near-field optics: Microscopy, spectroscopy, and surface modification beyond the diffraction limit, *Science* 257(5067), 189 (1992)
 54. T. J. Silva and S. Schultz, A scanning near-field optical microscope for the imaging of magnetic domains in reflection, *Rev. Sci. Instrum.* 67(3), 715 (1996)
 55. F. Matthes, H. Bruckl, and G. Reiss, Near-field magneto-optical microscopy in collection and illumination mode, *Ultramicroscopy* 71(1–4), 243 (1998)
 56. P. Bertrand, L. Conin, C. Hermann, G. Lampel, J. Peretti, and V. I. Safarov, Imaging of magnetic domains with scanning tunneling optical microscopy, *J. Appl. Phys.* 83(11), 6834 (1998)
 57. C. Durkan, I. V. Shvets, and J. C. Lodder, Observation of magnetic domains using a reflection-mode scanning near-field optical microscope, *Appl. Phys. Lett.* 70(10), 1323 (1997)
 58. S. Takahashi, W. Dickson, R. Pollard, and A. Zayats, Near-field magneto-optical analysis in reflection mode SNOM, *Ultramicroscopy* 100(3–4), 443 (2004)
 59. P. Fumagalli, A. Rosenberger, G. Eggers, A. Munnemann, N. Held, and G. Guntherodt, Quantitative determination of the local Kerr rotation by scanning near-field magneto-optic microscopy, *Appl. Phys. Lett.* 72(22), 2803 (1998)
 60. S. Grésillon, H. Cory, J. C. Rivoal, and A. C. Boccara, Transmission-mode apertureless near-field microscope: Optical and magneto-optical studies, *J. Opt. A* 1(2), 178 (1999)
 61. J. N. Walford, J. A. Porto, R. Carminati, and J. J. Greffet, Theory of near-field magnetooptical imaging, *J. Opt. Soc. Am. A* 19(3), 572 (2002)
 62. P. Fumagalli, Scanning near-field magneto-optic microscopy, in: Modern Techniques for Characterizing Magnetic Materials, edited by Y. Zhu, Dordrecht: Springer, 2005, pp 455–515
 63. S. Sugano and N. Kojima (Eds.), Magneto-Optics (Springer Series in Solid-State Sciences), Berlin: Springer, 2000
 64. W. Dickson, S. Takahashi, R. Pollard, R. Atkinson, and A. V. Zayats, Near-field imaging of ultrathin magnetic films with in-plane magnetization, *Journal of Microscopy* 209(3), 194 (2003)
 65. A. Kapitulnik, J. S. Dodge, and M. M. Fejer, High-resolution magneto-optic measurements with a Sagnac interferometer, *J. Appl. Phys.* 75(10), 6872 (1994)
 66. B. L. Petersen, A. Bauer, G. Meyer, T. Crecelius, and G. Kaindl, Kerr-rotation imaging in scanning near-field optical microscopy using a modified Sagnac interferometer, *Appl. Phys. Lett.* 73(4), 538 (1998)
 67. I. I. Smolyaninov, A. V. Zayats, and C. C. Davis, Near-field second-harmonic imaging of ferromagnetic and ferroelectric materials, *Opt. Lett.* 22(21), 1592 (1997)
 68. D. Wegner, U. Conrad, J. Gudde, G. Meyer, T. Crecelius, and A. Bauer, In-plane magnetization of garnet films imaged by proximal probe nonlinear magneto-optical microscopy, *J. Appl. Phys.* 88(4), 2166 (2000)
 69. W. Dickson, S. Takahashi, C. M. I. Boronat, R. M. Bowman, J. M. Gregg, and A. V. Zayats, Near-field second-harmonic imaging of thin ferroelectric films, *Phys. Rev. B* 72(9), 094110 (2005)
 70. J. Stadler, T. Schmid, and R. Zenobi, Developments in and practical guidelines for tip-enhanced Raman spectroscopy, *Nanoscale* 4(6), 1856 (2012)
 71. T. Mino, Y. Saito, and P. Verma, Quantitative analysis of polarization-controlled tip-enhanced Raman imaging through the evaluation of the tip dipole, *ACS Nano* 8(10), 10187 (2014)
 72. Y. Saito and P. Verma, Polarization-controlled Raman microscopy and nanoscopy, *J. Phys. Chem. Lett.* 3(10), 1295 (2012)
 73. M. D. Sonntag, E. A. Pozzi, N. Jiang, M. C. Hersam, and R. P. Van Duyne, Recent advances in tip-enhanced Raman spectroscopy, *J. Phys. Chem. Lett.* 5(18), 3125 (2014)
 74. P. Verma, T. Ichimura, T. Yano, Y. Saito, and S. Kawata, Nano-imaging through tip-enhanced Raman spectroscopy: Stepping beyond the classical limits, *Laser Photonics Rev.* 4(4), 548 (2010)
 75. T. Mino, Y. Saito, H. Yoshida, S. Kawata, and P. Verma, Molecular orientation analysis of organic thin films by z -polarization Raman microscope, *J. Raman Spectrosc.* 43(12), 2029 (2012)
 76. H. A. Bethe, Theory of diffraction by small holes, *Phys. Rev.* 66(7–8), 163 (1944)
 77. L. Novotny and C. Hafner, Light propagation in a cylindrical waveguide with a complex, metallic, dielectric function, *Phys. Rev. E* 50(5), 4094 (1994)
 78. R. D. Grober, T. Rutherford, and T. D. Harris, Modal approximation for the electromagnetic field of a near-field optical probe, *Appl. Opt.* 35(19), 3488 (1996)
 79. Th. Huser, L. Novotny, Th. Lacoste, R. Eckert, and H. Heinzelmann, Observation and analysis of near-field optical diffraction, *J. Opt. Soc. Am. A* 16(1), 141 (1999)
 80. T. Kalkbrenner, M. Ramstein, J. Mlynek, and V. Sandoghdar, A single gold particle as a probe for apertureless scanning near-field optical microscopy, *Journal of Microscopy-Oxford* 202(1), 72 (2001)
 81. M. I. Stockman, Nanofocusing of optical energy in tapered plasmonic waveguides, *Phys. Rev. Lett.* 93(13), 137404 (2004)

82. F. Huth, M. Schnell, J. Wittborn, N. Ocelic, and R. Hillenbrand, Infrared-spectroscopic nanoimaging with a thermal source, *Nat. Mater.* 10(5), 352 (2011)
83. J. Stadler, T. Schmid, and R. Zenobi, Nanoscale chemical imaging using top-illumination tip-enhanced Raman spectroscopy, *Nano Lett.* 10(11), 4514 (2010)
84. A. Weber-Bargioni, A. Schwartzberg, M. Cornaglia, A. Ismach, J. J. Urban, Y. Pang, R. Gordon, J. Bokor, M. B. Salmeron, D. F. Ogletree, P. Ashby, S. Cabrini, and P. J. Schuck, Hyperspectral nanoscale imaging on dielectric substrates with coaxial optical antenna scan probes, *Nano Lett.* 11(3), 1201 (2011)
85. P. G. Gucciardi, M. Lopes, R. Déturche, C. Julien, D. Barchiesi, and M. L. de la Chapelle, Light depolarization induced by metallic tips in apertureless near-field optical microscopy and tip-enhanced Raman spectroscopy, *Nanotechnology* 19(21), 215702 (2008)
86. R. Ossikowski, Q. Nguyen, and G. Picardi, Simple model for the polarization effects in tip-enhanced Raman spectroscopy, *Phys. Rev. B* 75(4), 045412 (2007)
87. T. Schmid, L. Opilik, C. Blum, and R. Zenobi, Nanoscale chemical imaging using tip-enhanced Raman spectroscopy: A critical review, *Angew. Chem. Int. Ed.* 52(23), 5940 (2013)
88. T. Schmid, B. S. Yeo, G. Leong, J. Stadler, and R. Zenobi, Performing tip-enhanced Raman spectroscopy in liquids, *J. Raman Spectrosc.* 40(10), 1392 (2009)
89. A. Tarun, N. Hayazawa, and S. Kawata, Tip-enhanced Raman spectroscopy for nanoscale strain characterization, *Anal. Bioanal. Chem.* 394(7), 1775 (2009)
90. Y. Ogawa, T. Toizumi, F. Minami, and A. V. Baranov, Nanometer-scale mapping of the strain and Ge content of Ge/Si quantum dots using enhanced Raman scattering by the tip of an atomic force microscope, *Phys. Rev. B* 83(8), 081302 (2011)
91. S. Nakashima, T. Mitani, M. Ninomiya, and K. Matsumoto, Raman investigation of strain in Si/SiGe heterostructures: Precise determination of the strain-shift coefficient of Si bands, *J. Appl. Phys.* 99(5), 053512 (2006)
92. R. M. Stöckle, Y. D. Suh, V. Deckert, and R. Zenobi, Nanoscale chemical analysis by tip-enhanced Raman spectroscopy, *Chem. Phys. Lett.* 318(1–3), 131 (2000)
93. Y. D. Suh, R. M. Soeckle, V. Deckert, and R. Zenobi, *Abstracts of Papers of the American Chemical Society* 221, U91 (2001)
94. E. Poliani, M. R. Wagner, J. S. Reparaz, M. Mandl, M. Strassburg, X. Kong, A. Trampert, C. M. Sotomayor Torres, A. Hoffmann, and J. Maultzsch, Nanoscale imaging of InN segregation and polymorphism in single vertically aligned InGaN/GaN multi quantum well nanorods by tip-enhanced Raman scattering, *Nano Lett.* 13(7), 3205 (2013)
95. S. Berweger, J. M. Atkin, R. L. Olmon, and M. B. Raschke, Adiabatic tip-plasmon focusing for nano-Raman spectroscopy, *J. Phys. Chem. Lett.* 1(24), 3427 (2010)
96. N. Hayazawa, M. Motohashi, Y. Saito, H. Ishitobi, A. Ono, T. Ichimura, P. Verma, and S. Kawata, Visualization of localized strain of a crystalline thin layer at the nanoscale by tip-enhanced Raman spectroscopy and microscopy, *J. Raman Spectrosc.* 38(6), 684 (2007)
97. C. Chen, N. Hayazawa, and S. Kawata, A 1.7 nm resolution chemical analysis of carbon nanotubes by tip-enhanced Raman imaging in the ambient, *Nat. Commun.* 5, 3312 (2014)
98. T. Yano, P. Verma, Y. Saito, T. Ichimura, and S. Kawata, Pressure-assisted tip-enhanced Raman imaging at a resolution of a few nanometres, *Nat. Photonics* 3(8), 473 (2009)
99. R. Zhang, Y. Zhang, Z. C. Dong, S. Jiang, C. Zhang, L. G. Chen, L. Zhang, Y. Liao, J. Aizpurua, Y. Luo, J. L. Yang, and J. G. Hou, Chemical mapping of a single molecule by plasmon-enhanced Raman scattering, *Nature* 498(7452), 82 (2013)
100. T. X. Huang, S. C. Huang, M. H. Li, Z. C. Zeng, X. Wang, and B. Ren, Tip-enhanced Raman spectroscopy: Tip-related issues, *Anal. Bioanal. Chem.* 407(27), 8177 (2015)
101. X. Zheng, C. Zong, M. Xu, X. Wang, and B. Ren, Raman imaging from microscopy to nanoscopy, and to macroscopy, *Small* 11(28), 3395 (2015)
102. R. Beams, L. G. Cancado, S. H. Oh, A. Jorio, and L. Novotny, Spatial coherence in near-field Raman scattering, *Phys. Rev. Lett.* 113(18), 186101 (2014)
103. F. De Angelis, G. Das, P. Candeloro, M. Patrini, M. Galli, A. Bek, M. Lazzarino, I. Maksymov, C. Liberale, L. C. Andreani, and E. Di Fabrizio, Nanoscale chemical mapping using three-dimensional adiabatic compression of surface plasmon polaritons, *Nat. Nanotechnol.* 5(1), 67 (2010)
104. A. Hartschuh, E. J. Sanchez, X. S. Xie, and L. Novotny, High-resolution near-field Raman microscopy of single-walled carbon nanotubes, *Phys. Rev. Lett.* 90(9), 095503 (2003)
105. M. Brehm, T. Taubner, R. Hillenbrand, and F. Keilmann, Infrared spectroscopic mapping of single nanoparticles and viruses at nanoscale resolution, *Nano Lett.* 6(7), 1307 (2006)
106. F. Huth, A. Govyadinov, S. Amarie, W. Nuansing, F. Keilmann, and R. Hillenbrand, Nano-FTIR absorption spectroscopy of molecular fingerprints at 20 nm spatial resolution, *Nano Lett.* 12(8), 3973 (2012)
107. A. C. Jones and M. B. Raschke, Thermal infrared near-field spectroscopy, *Nano Lett.* 12(3), 1475 (2012)
108. I. Amenabar, S. Poly, W. Nuansing, E. H. Hubrich, A. A. Govyadinov, F. Huth, R. Krutokhvostov, L. Zhang, M. Knez, J. Heberle, A. M. Bittner, and R. Hillenbrand, Structural analysis and mapping of individual protein complexes by infrared nanospectroscopy, *Nat. Commun.* 4, 2890 (2013)
109. H. A. Bechtel, E. A. Muller, R. L. Olmon, M. C. Martin, and M. B. Raschke, Ultrabroadband infrared nanospectroscopic imaging, *Proc. Natl. Acad. Sci. USA* 111(20), 7191 (2014)
110. S. Mastel, A. A. Govyadinov, T. V. A. G. de Oliveira, I. Amenabar, and R. Hillenbrand, Nanoscale-resolved chemi-

- cal identification of thin organic films using infrared near-field spectroscopy and standard Fourier transform infrared references, *Appl. Phys. Lett.* 106(2), 023113 (2015)
111. B. Pollard, E. A. Muller, K. Hinrichs, and M. B. Raschke, Vibrational nano-spectroscopic imaging correlating structure with intermolecular coupling and dynamics, *Nat. Commun.* 5, 3587 (2014)
112. C. Höppener and L. Novotny, Exploiting the light–metal interaction for biomolecular sensing and imaging, *Q. Rev. Biophys.* 45(02), 209 (2012)
113. B. D. Mangum, C. Mu, and J. M. Gerton, Resolving single fluorophores within dense ensembles: Contrast limits of tip-enhanced fluorescence microscopy, *Opt. Express* 16(9), 6183 (2008)
114. B. D. Mangum, E. Shafran, C. Mu, and J. M. Gerton, Three-dimensional mapping of near-field interactions via single-photon tomography, *Nano Lett.* 9(10), 3440 (2009)
115. L. Neumann, Y. J. Pang, A. Houyou, M. L. Juan, R. Gordon, and N. F. van Hulst, Extraordinary optical transmission brightens near-field fiber probe, *Nano Lett.* 11(2), 355 (2011)
116. M. A. Bopp, A. J. Meixner, G. Tarrach, I. Zschokke-Gränacher, and L. Novotny, Direct imaging single molecule diffusion in a solid polymer host, *Chem. Phys. Lett.* 263(6), 721 (1996)
117. T. W. Johnson, Z. J. Lapin, R. Beams, N. C. Lindquist, S. G. Rodrigo, L. Novotny, and S. H. Oh, Highly reproducible near-field optical imaging with sub-20-nm resolution based on template-stripped gold pyramids, *ACS Nano* 6(10), 9168 (2012)
118. C. C. Neacsu, G. A. Reider, and M. B. Raschke, Second-harmonic generation from nanoscopic metal tips: Symmetry selection rules for single asymmetric nanostructures, *Phys. Rev. B* 71(20), 201402 (2005)
119. A. L. Demming, F. Festy, and D. Richards, Plasmon resonances on metal tips: Understanding tip-enhanced Raman scattering, *J. Chem. Phys.* 122(18), 184716 (2005)
120. D. Mehtani, N. Lee, R. D. Hartschuh, A. Kisliuk, M. D. Foster, A. P. Sokolov, and J. F. Maguire, Nano-Raman spectroscopy with side-illumination optics, *J. Raman Spectrosc.* 36(11), 1068 (2005)
121. J. A. Veerman, M. F. Garcia-Parajo, L. Kuipers, and N. F. Van Hulst, Single molecule mapping of the optical field distribution of probes for near-field microscopy, *Journal of Microscopy* 194(2–3), 477 (1999)
122. B. Sick, B. Hecht, U. P. Wild, and L. Novotny, Probing confined fields with single molecules and vice versa, *Journal of Microscopy* 202(2), 365 (2001)
123. K. G. Lee, H. W. Kihm, K. J. Ahn, J. S. Ahn, Y. D. Suh, C. Lienau, and D. S. Kim, Vector field mapping of local polarization using gold nanoparticle functionalized tips: Independence of the tip shape, *Opt. Express* 15(23), 14993 (2007)
124. C. Huang, A. Bouhelier, G. Colas des Francs, A. Bruyant, A. Guenot, E. Finot, J. C. Weeber, and A. Dereux, Gain, detuning, and radiation patterns of nanoparticle optical antennas, *Phys. Rev. B* 78(15), 155407 (2008)
125. M. A. Lieb, J. M. Zavislan, and L. Novotny, Single-molecule orientations determined by direct emission pattern imaging, *J. Opt. Soc. Am. B* 21(6), 1210 (2004)
126. T. H. Tamini, F. D. Stefani, F. B. Segerink, and N. F. Van Hulst, Optical antennas direct single-molecule emission, *Nat. Photonics* 2(4), 234 (2008)
127. S. Kuhn, G. Mori, M. Agio, and V. Sandoghdar, Modification of single molecule fluorescence close to a nanostructure: Radiation pattern, spontaneous emission and quenching, *Mol. Phys.* 106(7), 893 (2008)
128. M. Böhmler, N. Hartmann, C. Georgi, F. Hennrich, A. A. Green, M. C. Hersam, and A. Hartschuh, Enhancing and redirecting carbon nanotube photoluminescence by an optical antenna, *Opt. Express* 18(16), 16443 (2010)
129. T. H. Tamini, S. Karaveli, N. F. van Hulst, and R. Zia, Quantifying the magnetic nature of light emission, *Nat. Commun.* 3, 979 (2012)
130. A. G. Curto, G. Volpe, T. H. Tamini, M. P. Kreuzer, R. Quidant, and N. F. van Hulst, Unidirectional emission of a quantum dot coupled to a nanoantenna, *Science* 329(5994), 930 (2010)
131. M. Terrones, Science and technology of the twenty-first century: Synthesis, properties, and applications of carbon nanotubes, *Annu. Rev. Mater. Res.* 33(1), 419 (2003)
132. M. S. Dresselhaus, A. Jorio, and R. Saito, Characterizing graphene, graphite, and carbon nanotubes by Raman spectroscopy, *Ann. Rev. Condens. Matter Phys.* 1, 89 (2010)
133. X. Zhang, W. Zhang, L. Liu, and Z. X. Shen, Surface-enhanced Raman of Z-vibration mode in single-walled and multi-walled carbon nanotube, *Chem. Phys. Lett.* 372(3–4), 497 (2003)
134. M. S. Dresselhaus, G. Dresselhaus, R. Saito, and A. Jorio, Raman spectroscopy of carbon nanotubes, *Phys. Rep.* 409(2), 47 (2005)
135. M. S. Dresselhaus, G. Dresselhaus, and A. Jorio, Raman spectroscopy of carbon nanotubes in 1997 and 2007, *J. Phys. Chem. C* 111(48), 17887 (2007)
136. C. Fantini, A. Jorio, M. Souza, M. S. Strano, M. S. Dresselhaus, and M. A. Pimenta, Optical transition energies for carbon nanotubes from resonant Raman spectroscopy: Environment and temperature effects, *Phys. Rev. Lett.* 93(14), 147406 (2004)
137. C. Fantini, A. Jorio, M. Souza, R. Saito, G. G. Samsonidze, M. S. Dresselhaus, and M. A. Pimenta, Steplike dispersion of the intermediate-frequency Raman modes in semiconducting and metallic carbon nanotubes, *Phys. Rev. B* 72(8), 085446 (2005)
138. R. Saito, T. Takeya, T. Kimura, G. Dresselhaus, and M. S. Dresselhaus, Finite-size effect on the Raman spectra of carbon nanotubes, *Phys. Rev. B* 59(3), 2388 (1999)

139. K. Sbai, A. Rahmani, H. Chadli, and J. L. Sauvajol, Finite-size effect on the Raman-active modes of double-walled carbon nanotubes, *J. Phys.: Condens. Matter* 20(1), 015204 (2008)
140. M. Mitra, and S. Gopalakrishnan, Vibrational characteristics of single-walled carbon-nanotube: Time and frequency domain analysis, *J. Appl. Phys.* 101(11), 114320 (2007)
141. G. Picardi, M. Chaigneau, and R. Ossikovski, High resolution probing of multi wall carbon nanotubes by Tip Enhanced Raman Spectroscopy in gap-mode, *Chem. Phys. Lett.* 469(1–3), 161 (2009)
142. I. O. Maciel, N. Anderson, M. A. Pimenta, A. Hartschuh, H. H. Qian, M. Terrones, H. Terrones, J. Campos-Delgado, A. M. Rao, L. Novotny, and A. Jorio, Electron and phonon renormalization near charged defects in carbon nanotubes, *Nat. Mater.* 7(11), 878 (2008)
143. N. Anderson, A. Hartschuh, and L. Novotny, Chirality changes in carbon nanotubes studied with near-field raman spectroscopy, *Nano Lett.* 7(3), 577 (2007)
144. Y. Saito, P. Verma, K. Masui, Y. Inouye, and S. Kawata, Nano-scale analysis of graphene layers by tip-enhanced near-field Raman spectroscopy, *J. Raman Spectrosc.* 40(10), 1434 (2009)
145. R. H. Rickman and P. R. Dunstan, Enhancement of lattice defect signatures in graphene and ultrathin graphite using tip-enhanced Raman spectroscopy, *J. Raman Spectrosc.* 45(1), 15 (2014)
146. R. Beams, L. G. Cancado, A. Jorio, A. N. Vamivakas, and L. Novotny, Tip-enhanced Raman mapping of local strain in graphene, *Nanotechnology* 26(17), 175702 (2015)
147. A. Shiotari, T. Kumagai, and M. Wolf, Tip-enhanced Raman spectroscopy of graphene nanoribbons on Au(111), *J. Phys. Chem. C* 118(22), 11806 (2014)
148. Z. Fei, A. S. Rodin, G. O. Andreev, W. Bao, A. S. McLeod, M. Wagner, L. M. Zhang, Z. Zhao, M. Thiemens, G. Dominguez, M. M. Fogler, A. H. C. Neto, C. N. Lau, F. Keilmann, and D. N. Basov, Gate-tuning of graphene plasmons revealed by infrared nano-imaging, *Nature* 487(7405), 82 (2012)
149. J. N. Chen, M. Badioli, P. Alonso-Gonzalez, S. Thongrattanasiri, F. Huth, J. Osmond, M. Spasenovic, A. Centeno, A. Pesquera, P. Godignon, A. Z. Elorza, N. Camara, F. J. G. de Abajo, R. Hillenbrand, and F. H. L. Koppens, Optical nano-imaging of gate-tunable graphene plasmons, *Nature* 487(7405), 77 (2012)
150. P. Alonso-Gonzalez, A. Y. Nikitin, F. Golmar, A. Centeno, A. Pesquera, S. Velez, J. Chen, G. Navickaite, F. Koppens, A. Zurutuza, F. Casanova, L. E. Hueso, and R. Hillenbrand, Controlling graphene plasmons with resonant metal antennas and spatial conductivity patterns, *Science* 344(6190), 1369 (2014)
151. A. Woessner, M. B. Lundeberg, Y. Gao, A. Principi, P. Alonso-González, M. Carrega, K. Watanabe, T. Taniguchi, G. Vignale, M. Polini, J. Hone, R. Hillenbrand, and F. H. L. Koppens, Highly confined low-loss plasmons in graphene–boron nitride heterostructures, *Nat. Mater.* 14(4), 421 (2015)
152. Z. Shi, X. Hong, H. A. Bechtel, B. Zeng, M. C. Martin, K. Watanabe, T. Taniguchi, Y. R. Shen, and F. Wang, Observation of a Luttinger-liquid plasmon in metallic single-walled carbon nanotubes, *Nat. Photonics* 9(8), 515 (2015)
153. M. Wagner, Z. Fei, A. S. McLeod, A. S. Rodin, W. Bao, E. G. Iwinski, Z. Zhao, M. Goldflam, M. Liu, G. Dominguez, M. Thiemens, M. M. Fogler, A. H. Castro Neto, C. N. Lau, S. Amarie, F. Keilmann, and D. N. Basov, Ultrafast and nanoscale plasmonic phenomena in exfoliated graphene revealed by infrared pump–probe nanoscopy, *Nano Lett.* 14(2), 894 (2014)
154. D. N. Basov, M. M. Fogler, A. Lanzara, F. Wang, and Y. Zhang, Colloquium: Graphene spectroscopy, *Rev. Mod. Phys.* 86(3), 959 (2014)
155. N. C. Lindquist, P. Nagpal, K. M. McPeak, D. J. Norris, and S. H. Oh, Engineering metallic nanostructures for plasmonics and nanophotonics, *Rep. Prog. Phys.* 75(3), 036501 (2012)
156. M. Fleischer, A. Weber-Bargioni, M. V. P. Altoe, A. M. Schwartzberg, P. J. Schuck, S. Cabrini, and D. P. Kern, Gold nanocone near-field scanning optical microscopy probes, *ACS Nano* 5(4), 2570 (2011)
157. P. Muhlschlegel, H. J. Eisler, O. J. F. Martin, B. Hecht, and D. W. Pohl, Resonant optical antennas, *Science* 308(5728), 1607 (2005)
158. P. J. Schuck, D. P. Fromm, A. Sundaramurthy, G. S. Kino, and W. E. Moerner, Improving the mismatch between light and nanoscale objects with gold Bowtie nanoantennas, *Phys. Rev. Lett.* 94(1), 017402 (2005)
159. D. P. Fromm, A. Sundaramurthy, P. J. Schuck, G. Kino, and W. E. Moerner, Gap-dependent optical coupling of single “Bowtie” nanoantennas resonant in the visible, *Nano Lett.* 4(5), 957 (2004)
160. P. Biagioni, J. S. Huang, and B. Hecht, Nanoantennas for visible and infrared radiation, *Rep. Prog. Phys.* 75(2), 024402 (2012)
161. J. N. Farahani, H. J. Eisler, D. W. Pohl, M. Pavius, P. Fluckiger, P. Gasser, and B. Hecht, Bow-tie optical antenna probes for single-emitter scanning near-field optical microscopy, *Nanotechnology* 18(12), 125506 (2007)
162. A. Weber-Bargioni, A. Schwartzberg, M. Schmidt, B. Harteneck, D. F. Ogletree, P. J. Schuck, and S. Cabrini, Functional plasmonic antenna scanning probes fabricated by induced-deposition mask lithography, *Nanotechnology* 21(6), 065306 (2010)
163. M. Melli, A. Polyakov, D. Gargas, C. Huynh, L. Scipioni, W. Bao, D. F. Ogletree, P. J. Schuck, S. Cabrini, and A. Weber-Bargioni, Reaching the theoretical resonance quality factor limit in coaxial plasmonic nanoresonators fabricated by helium ion lithography, *Nano Lett.* 13(6), 2687 (2013)

164. B. Radisavljevic, A. Radenovic, J. Brivio, V. Giacometti, and A. Kis, Single-layer MoS₂ transistors, *Nat. Nanotechnol.* 6(3), 147 (2011)
165. Q. H. Wang, K. Kalantar-Zadeh, A. Kis, J. N. Coleman, and M. S. Strano, Electronics and optoelectronics of two-dimensional transition metal dichalcogenides, *Nat. Nanotechnol.* 7(11), 699 (2012)
166. Z. Yin, H. Li, H. Li, L. Jiang, Y. Shi, Y. Sun, G. Lu, Q. Zhang, X. Chen, and H. Zhang, Single-layer MoS₂ phototransistors, *ACS Nano* 6(1), 74 (2012)
167. J. S. Ross, P. Klement, A. M. Jones, N. J. Ghimire, J. Yan, D. G. Mandrus, T. Taniguchi, K. Watanabe, K. Kitamura, W. Yao, D. H. Cobden, and X. Xu, Electrically tunable excitonic light-emitting diodes based on monolayer WSe₂ p-n junctions, *Nat. Nanotechnol.* 9(4), 268 (2014)
168. W. Wu, L. Wang, Y. Li, F. Zhang, L. Lin, S. Niu, D. Chenet, X. Zhang, Y. Hao, T. F. Heinz, J. Hone, and Z. L. Wang, Piezoelectricity of single-atomic-layer MoS₂ for energy conversion and piezotronics, *Nature* 514(7523), 470 (2014)
169. B. W. H. Baugher, H. O. H. Churchill, Y. Yang, and P. Jarillo-Herrero, Optoelectronic devices based on electrically tunable p-n diodes in a monolayer dichalcogenide, *Nat. Nanotechnol.* 9(4), 262 (2014)
170. F. H. L. Koppens, T. Mueller, P. Avouris, A. C. Ferrari, M. S. Vitiello, and M. Polini, Photodetectors based on graphene, other two-dimensional materials and hybrid systems, *Nat. Nanotechnol.* 9(10), 780 (2014)
171. G. Fiori, F. Bonaccorso, G. Iannaccone, T. Palacios, D. Neumaier, A. Seabaugh, S. K. Banerjee, and L. Colombo, Electronics based on two-dimensional materials, *Nat. Nanotechnol.* 9(10), 768 (2014)
172. F. Xia, H. Wang, D. Xiao, M. Dubey, and A. Ramasubramaniam, Two-dimensional material nanophotonics, *Nat. Photonics* 8(12), 899 (2014)
173. K. S. Novoselov, A. K. Geim, S. V. Morozov, D. Jiang, M. I. Katsnelson, I. V. Grigorieva, S. V. Dubonos, and A. A. Firsov, Two-dimensional gas of massless Dirac fermions in graphene, *Nature* 438(7065), 197 (2005)
174. Y. B. Zhang, Y. W. Tan, H. L. Stormer, and P. Kim, Experimental observation of the quantum Hall effect and Berry's phase in graphene, *Nature* 438(7065), 201 (2005)
175. K. F. Mak, C. Lee, J. Hone, J. Shan, and T. F. Heinz, Atomically thin MoS₂: A new direct-gap semiconductor, *Phys. Rev. Lett.* 105(13), 136805 (2010)
176. A. Splendiani, L. Sun, Y. Zhang, T. Li, J. Kim, C. Y. Chim, G. Galli, and F. Wang, Emerging photoluminescence in monolayer MoS₂, *Nano Lett.* 10(4), 1271 (2010)
177. A. Chernikov, T. C. Berkelbach, H. M. Hill, A. Rigos, Y. Li, O. B. Aslan, D. R. Reichman, M. S. Hybertsen, and T. F. Heinz, Exciton binding energy and nonhydrogenic Rydberg series in monolayer WS₂, *Phys. Rev. Lett.* 113(7), 076802 (2014)
178. Z. Ye, T. Cao, K. O'Brien, H. Zhu, X. Yin, Y. Wang, S. G. Louie, and X. Zhang, Probing excitonic dark states in single-layer tungsten disulphide, *Nature* 513(7517), 214 (2014)
179. X. Xu, W. Yao, D. Xiao, and T. F. Heinz, Spin and pseudospins in layered transition metal dichalcogenides, *Nat. Phys.* 10(5), 343 (2014)
180. A. K. Geim and I. V. Grigorieva, Van der Waals heterostructures, *Nature* 499(7459), 419 (2013)
181. S. Z. Butler, S. M. Hollen, L. Cao, Y. Cui, J. A. Gupta, H. R. Gutierrez, T. F. Heinz, S. S. Hong, J. Huang, A. F. Ismach, E. Johnston-Halperin, M. Kuno, V. V. Plashnitsa, R. D. Robinson, R. S. Ruoff, S. Salahuddin, J. Shan, L. Shi, M. G. Spencer, M. Terrones, W. Windl, and J. E. Goldberger, Progress, challenges, and opportunities in two-dimensional materials beyond graphene, *ACS Nano* 7(4), 2898 (2013)
182. K. F. Mak, K. He, C. Lee, G. H. Lee, J. Hone, T. F. Heinz, and J. Shan, Tightly bound trions in monolayer MoS₂, *Nat. Mater.* 12(3), 207 (2013)
183. C. Zhang, A. Johnson, C. L. Hsu, L. J. Li, and C. K. Shih, Direct imaging of band profile in single layer MoS₂ on graphite: Quasiparticle energy gap, metallic edge states, and edge band bending, *Nano Lett.* 14(5), 2443 (2014)
184. M. M. Ugeda, A. J. Bradley, S. F. Shi, F. H. da Jornada, Y. Zhang, D. Y. Qiu, W. Ruan, S. K. Mo, Z. Hussain, Z. X. Shen, F. Wang, S. G. Louie, and M. F. Crommie, Giant bandgap renormalization and excitonic effects in a monolayer transition metal dichalcogenide semiconductor, *Nat. Mater.* 13(12), 1091 (2014)
185. W. Zhu, T. Low, Y.H. Lee, H. Wang, D. B. Farmer, J. Kong, F. Xia, and P. Avouris, Electronic transport and device prospects of monolayer molybdenum disulphide grown by chemical vapour deposition, *Nat. Commun.* 5, 3087 (2014)
186. J. A. Schuller, S. Karaveli, T. Schiros, K. He, S. Yang, I. Kymissis, J. Shan, and R. Zia, Orientation of luminescent excitons in layered nanomaterials, *Nat. Nanotechnol.* 8(4), 271 (2013)
187. D. F. Ogletree, P. J. Schuck, A. F. Weber-Bargioni, N. J. Borys, S. Aloni, W. Bao, S. Barja, J. Lee, M. Melli, K. Munechika, S. Whitelam, and S. Wickenburg, Revealing optical properties of reduced-dimensionality materials at relevant length scales, *Adv. Mater.* 27(38), 5693 (2015)
188. Y. Abate, S. Gamage, L. Zhen, S. B. Cronin, H. Wang, V. Babicheva, M. H. Javani, and M. I. Stockman, Nanoscopy reveals metallic black phosphorus, arXiv: 1506.05431
189. Y. Lee, S. Park, H. Kim, G. H. Han, Y. H. Lee, and J. Kim, Characterization of the structural defects in CVD-grown monolayered MoS₂ using near-field photoluminescence imaging, *Nanoscale* 7(28), 11909 (2015)
190. Y. Kang, S. Najmaei, Z. Liu, Y. Bao, Y. Wang, X. Zhu, N. J. Halas, P. Nordlander, P. M. Ajayan, J. Lou, and Z. Fang, Plasmonic hot electron induced structural phase transition in a MoS₂ monolayer, *Adv. Mater.* 26(37), 6467 (2014)
191. W. Bao, M. Melli, N. Caselli, F. Riboli, D. S. Wiersma, M. Staffaroni, H. Choo, D. F. Ogletree, S. Aloni, J. Bokor, S. Cabrini, F. Intonti, M. B. Salmeron, E. Yablonovitch, P.

REVIEW ARTICLE

- J. Schuck, and A. Weber-Bargioni, Mapping local charge recombination heterogeneity by multidimensional nanospectroscopic imaging, *Science* 338(6112), 1317 (2012)
192. W. Bao, M. Staffaroni, J. Bokor, M. B. Salmeron, E. Yablonovitch, S. Cabrini, A. Weber-Bargioni, and P. J. Schuck, Plasmonic near-field probes: A comparison of the campanile geometry with other sharp tips, *Opt. Express* 21(7), 8166 (2013)
193. W. Bao, N. J. Borys, C. Ko, J. Suh, W. Fan, A. Thron, Y. Zhang, A. Buynanin, J. Zhang, S. Cabrini, P. D. Ashby, A. Weber-Bargioni, S. Tongay, S. Aloni, D. F. Ogletree, J. Wu, M. B. Salmeron, and P. J. Schuck, Visualizing nanoscale excitonic relaxation properties of disordered edges and grain boundaries in monolayer molybdenum disulfide, *Nat. Commun.* 6, 7993 (2015)
194. X. Cui, G. H. Lee, Y. D. Kim, G. Arefe, P. Y. Huang, C. H. Lee, D. A. Chenet, X. Zhang, L. Wang, F. Ye, F. Pizzocchero, B. S. Jessen, K. Watanabe, T. Taniguchi, D. A. Muller, T. Low, P. Kim, and J. Hone, Multi-terminal transport measurements of MoS₂ using a van der Waals heterostructure device platform, *Nat. Nanotechnol.* 10(6), 534 (2015)
195. E. Devaux, A. Dereux, E. Bourillot, J. C. Weeber, Y. Lacroute, J. P. Goudonnet, and C. Girard, Local detection of the optical magnetic field in the near zone of dielectric samples, *Phys. Rev. B* 62(15), 10504 (2000)
196. Z. H. Kim and S. R. Leone, Polarization-selective mapping of near-field intensity and phase around gold nanoparticles using apertureless near-field microscopy, *Opt. Express* 16(3), 1733 (2008)
197. D. S. Kim, J. Heo, S. H. Ahn, S. W. Han, W. S. Yun, and Z. H. Kim, Real-space mapping of the strongly coupled plasmons of nanoparticle dimers, *Nano Lett.* 9(10), 3619 (2009)
198. M. Schnell, A. Garcia-Etxarri, A. J. Huber, K. Crozier, J. Aizpurua, and R. Hillenbrand, Controlling the near-field oscillations of loaded plasmonic nanoantennas, *Nat. Photonics* 3(5), 287 (2009)
199. M. Schnell, P. Alonso-Gonzalez, L. Arzubiaga, F. Casanova, L. E. Hueso, A. Chuvalin, and R. Hillenbrand, Nanofocusing of mid-infrared energy with tapered transmission lines, *Nat. Photonics* 5(5), 283 (2011)
200. R. L. Olmon, M. Rang, P. M. Krenz, B. A. Lail, L. V. Saraf, G. D. Boreman, and M. B. Raschke, Determination of electric-field, magnetic-field, and electric-current distributions of infrared optical antennas: A near-field optical vector network analyzer, *Phys. Rev. Lett.* 105(16), 167403 (2010)
201. R. L. Olmon, P. M. Krenz, A. C. Jones, G. D. Boreman, and M. B. Raschke, Near-field imaging of optical antenna modes in the mid-infrared, *Opt. Express* 16(25), 20295 (2008)
202. N. Yu, E. Cubukcu, L. Diehl, M. A. Belkin, K. B. Crozier, F. Capasso, D. Bour, S. Corzine, and G. Hofler, Plasmonic quantum cascade laser antenna, *Appl. Phys. Lett.* 91(17), 173113 (2007)
203. L. Novotny and C. Henkel, Van der Waals versus optical interaction between metal nanoparticles, *Opt. Lett.* 33(9), 1029 (2008)
204. J. Dorfmüller, D. Dregely, M. Esslinger, W. Khunsin, R. Vogelgesang, K. Kern, and H. Giessen, Near-field dynamics of optical Yagi-Uda nanoantennas, *Nano Lett.* 11(7), 2819 (2011)
205. T. Zentgraf, J. Dorfmuller, C. Rockstuhl, C. Etrich, R. Vogelgesang, K. Kern, T. Pertsch, F. Lederer, and H. Giessen, Amplitude- and phase-resolved optical near fields of splitting-resonator-based metamaterials, *Opt. Lett.* 33(8), 848 (2008)
206. B. Deutsch, R. Hillenbrand, and L. Novotny, Visualizing the optical interaction tensor of a gold nanoparticle pair, *Nano Lett.* 10(2), 652 (2010)
207. H. A. Bechtel, J. P. Camden, Z. H. Kim, D. J. A. Brown, and R. N. Zare, *Abstracts of Papers of the American Chemical Society* 228, U275 (2004)
208. P. Alonso-Gonzalez, M. Schnell, P. Sarriugarte, H. Sobhani, C. Wu, N. Arju, A. Khanikaev, F. Golmar, P. Albella, L. Arzubiaga, F. Casanova, L. E. Hueso, P. Nordlander, G. Shvets, and R. Hillenbrand, Real-space mapping of fano interference in plasmonic metamolecules, *Nano Lett.* 11(9), 3922 (2011)
209. P. Uebel, M. A. Schmidt, H. W. Lee, and P. S. J. Russell, Polarisation-resolved near-field mapping of a coupled gold nanowire array, *Opt. Express* 20(27), 28409 (2012)
210. S. Mastel, S. E. Grefe, G. B. Cross, A. Taber, S. Dhuey, S. Cabrini, P. J. Schuck, and Y. Abate, Real-space mapping of nanoplasmonic hotspots via optical antenna-gap loading, *Appl. Phys. Lett.* 101(13), 131102 (2012)
211. S. E. Grefe, D. Leiva, S. Mastel, S. D. Dhuey, S. Cabrini, P. J. Schuck, and Y. Abate, Near-field spatial mapping of strongly interacting multiple plasmonic infrared antennas, *Phys. Chem. Chem. Phys.* 15(43), 18944 (2013)
212. T. Bauer, S. Orlov, U. Peschel, P. Banzer, and G. Leuchs, Nanointerferometric amplitude and phase reconstruction of tightly focused vector beams, *Nat. Photonics* 8(1), 23 (2014)
213. N. Ocelic, A. Huber, and R. Hillenbrand, Pseudoheterodyne detection for background-free near-field spectroscopy, *Appl. Phys. Lett.* 89(10), 101124 (2006)
214. M. L. M. Balistreri, J. P. Korterik, L. Kuipers, and N. F. van Hulst, Local observations of phase singularities in optical fields in waveguide structures, *Phys. Rev. Lett.* 85(2), 294 (2000)
215. A. Nesci, R. Dandliker, and H. P. Herzig, Quantitative amplitude and phase measurement by use of a heterodyne scanning near-field optical microscope, *Opt. Lett.* 26(4), 208 (2001)
216. E. Verhagen, M. Spasenovic, A. Polman, and L. Kuipers, Nanowire plasmon excitation by adiabatic mode transformation, *Phys. Rev. Lett.* 102(20), 203904 (2009)
217. M. Burresi, D. Diessel, D. Oosten, S. Linden, M. Wegener,

- and L. Kuipers, Negative-index metamaterials: Looking into the unit cell, *Nano Lett.* 10(7), 2480 (2010)
218. H. Gersen, T. J. Karle, R. J. P. Engelen, W. Bogaerts, J. P. Korterik, N. F. van Hulst, T. F. Krauss, and L. Kuipers, Direct observation of Bloch harmonics and negative phase velocity in photonic crystal waveguides, *Phys. Rev. Lett.* 94(12), 123901 (2005)
219. M. Ayache, M. P. Nezhad, S. Zamek, M. Abashin, and Y. Fainman, Near-field measurement of amplitude and phase in silicon waveguides with liquid cladding, *Opt. Lett.* 36(10), 1869 (2011)
220. M. Burresi, R. J. P. Engelen, A. Opheij, D. van Oosten, D. Mori, T. Baba, and L. Kuipers, Observation of polarization singularities at the nanoscale, *Phys. Rev. Lett.* 102(3), 033902 (2009)
221. N. Rotenberg, T. L. Krijger, B. Feber, M. Spasenović, F. J. G. de Abajo, and L. Kuipers, Magnetic and electric response of single subwavelength holes, *Phys. Rev. B* 88(24), 241408 (2013)
222. M. Burresi, D. van Oosten, T. Kampfrath, H. Schoenmaker, R. Heideman, A. Leinse, and L. Kuipers, Probing the magnetic field of light at optical frequencies, *Science* 326(5952), 550 (2009)
223. M. Burresi, T. Kampfrath, D. van Oosten, J. C. Prangsma, B. S. Song, S. Noda, and L. Kuipers, Magnetic light-matter interactions in a photonic crystal nanocavity, *Phys. Rev. Lett.* 105(12), 123901 (2010)
224. S. Vignolini, F. Intonti, F. Riboli, L. Balet, L. H. Li, M. Francardi, A. Gerardino, A. Fiore, D. S. Wiersma, and M. Gurioli, Magnetic imaging in photonic crystal microcavities, *Phys. Rev. Lett.* 105(12), 123902 (2010)
225. M. Spasenović, D. M. Beggs, P. Lalanne, T. F. Krauss, and L. Kuipers, Measuring the spatial extent of individual localized photonic states, *Phys. Rev. B* 86(15), 155153 (2012)
226. S. R. Huisman, G. Cstis, S. Stobbe, A. P. Mosk, J. L. Herek, A. Lagendijk, P. Lodahl, W. L. Vos, and P. W. H. Pinkse, Measurement of a band-edge tail in the density of states of a photonic-crystal waveguide, *Phys. Rev. B* 86(15), 155154 (2012)
227. D. Denkova, N. Verellen, A. V. Silhanek, V. K. Valev, P. V. Dorpe, and V. V. Moshchalkov, Mapping magnetic near-field distributions of plasmonic nanoantennas, *ACS Nano* 7(4), 3168 (2013)
228. D. Denkova, N. Verellen, A. V. Silhanek, P. Van Dorpe, and V. V. Moshchalkov, Lateral magnetic near-field imaging of plasmonic nanoantennas with increasing complexity, *Small* 10(10), 1959 (2014)
229. H. W. Kihm, S. M. Koo, Q. H. Kim, K. Bao, J. E. Kihm, W. S. Bak, S. H. Eah, C. Lienau, H. Kim, P. Nordlander, N. J. Halas, N. K. Park, and D. S. Kim, Bethe-hole polarization analyser for the magnetic vector of light, *Nat. Commun.* 2, 451 (2011)
230. H. W. Kihm, J. Kim, S. Koo, J. Ahn, K. Ahn, K. Lee, N. Park, and D. S. Kim, Optical magnetic field mapping using a subwavelength aperture, *Opt. Express* 21(5), 5625 (2013)
231. B. le Feber, N. Rotenberg, D. M. Beggs, and L. Kuipers, Simultaneous measurement of nanoscale electric and magnetic optical fields, *Nat. Photonics* 8(1), 43 (2014)
232. N. Caselli, F. La China, W. Bao, F. Riboli, A. Gerardino, L. Li, E. H. Linfield, F. Pagliano, A. Fiore, P. J. Schuck, S. Cabrini, A. Weber-Bargioni, M. Gurioli, and F. Intonti, Deep-subwavelength imaging of both electric and magnetic localized optical fields by plasmonic campanile nanoantenna, *Sci. Rep.* 5, 9606 (2015)
233. H. U. Yang, R. L. Olmon, K. S. Deryckx, X. G. Xu, H. A. Bechtel, Y. Xu, B. A. Lail, and M. B. Raschke, Accessing the optical magnetic near-field through Babinet's principle, *ACS Photonics* 1(9), 894 (2014)
234. L. Novotny, R. X. Bian, and X. S. Xie, Theory of nanometric optical tweezers, *Phys. Rev. Lett.* 79(4), 645 (1997)
235. J. Berthelot, S. S. Acimovic, M. L. Juan, M. P. Kreuzer, J. Renger, and R. Quidant, Three-dimensional manipulation with scanning near-field optical nanotweezers, *Nat. Nanotechnol.* 9(4), 295 (2014)
236. R. M. Gelfand, S. Wheaton, and R. Gordon, Cleaved fiber optic double nanohole optical tweezers for trapping nanoparticles, *Opt. Lett.* 39(22), 6415 (2014)
237. J. Jose, S. Kress, A. Barik, L. M. Otto, J. Shaver, T. W. Johnson, Z. J. Lapin, P. Bharadwaj, L. Novotny, and S. H. Oh, Individual template-stripped conductive gold pyramids for tip-enhanced dielectrophoresis, *ACS Photonics* 1(5), 464 (2014)
238. N. M. Hameed, A. El Eter, T. Grosjean, and F. I. Baida, Stand-alone three-dimensional optical tweezers based on fibred Bowtie nanoaperture, *IEEE Photonics J.* 6(4), 4500510 (2014)
239. S. Wheaton, R. M. Gelfand, and R. Gordon, Probing the Raman-active acoustic vibrations of nanoparticles with extraordinary spectral resolution, *Nat. Photonics* 9(1), 68 (2015)
240. A. A. Al Balushi and R. Gordon, A label-free Untethered approach to single-molecule protein binding kinetics, *Nano Lett.* 14(10), 5787 (2014)
241. H. K. Wickramasinghe, M. Chaigneau, R. Yasukuni, G. Picardi, and R. Ossikowski, Billion-fold increase in tip-enhanced Raman signal, *ACS Nano* 8(4), 3421 (2014)
242. I. Rajapaksa, K. Uenal, and H. K. Wickramasinghe, Image force microscopy of molecular resonance: A microscope principle, *Appl. Phys. Lett.* 97(7), 073121 (2010)
243. J. Jahng, J. Brocious, D. A. Fishman, F. Huang, X. Li, V. A. Tammar, H. K. Wickramasinghe, and E. O. Potma, Gradient and scattering forces in photoinduced force microscopy, *Phys. Rev. B* 90(15), 155417 (2014)
244. J. Jahng, J. Brocious, D. A. Fishman, S. Yampolsky, D. Nowak, F. Huang, V. A. Apkarian, H. K. Wickramasinghe, and E. O. Potma, Ultrafast pump-probe force microscopy with nanoscale resolution, *Appl. Phys. Lett.* 106(8), 083113 (2015)

245. R. M. Gelfand, A. Bonakdar, O. G. Memis, and H. Mohseni, Super resolution mapping of the near optical field and the gradient optical force, *Proc. SPIE 8815, Nanoimaging and Nanospectroscopy 8815*, 88150R (2013)
246. A. Giugni, B. Torre, A. Toma, M. Francardi, M. Malerba, A. Alabastri, R. P. Zaccaria, M. I. Stockman, and E. Di Fabrizio, Hot-electron nanoscopy using adiabatic compression of surface plasmons, *Nat. Nanotechnol.* 8(11), 845 (2013)
247. P. J. Schuck, Nanoimaging: Hot electrons go through the barrier, *Nat. Nanotechnol.* 8(11), 799 (2013)
248. A. O. Govorov, H. Zhang, and Y. K. Gun'ko, Theory of photoinjection of hot plasmonic carriers from metal nanostructures into semiconductors and surface molecules, *J. Phys. Chem. C* 117(32), 16616 (2013)
249. A. Polyakov, C. Senft, K. F. Thompson, J. Feng, S. Cabrini, P. J. Schuck, H. A. Padmore, S. J. Peppernick, and W. P. Hess, Plasmon-enhanced photocathode for high brightness and high repetition rate X-ray sources, *Phys. Rev. Lett.* 110(7), 076802 (2013)
250. W. A. Challener, C. Peng, A. V. Itagi, D. Karns, W. Peng, Y. Peng, X. Yang, X. Zhu, N. J. Gokemeijer, Y. T. Hsia, G. Ju, R. E. Rottmayer, M. A. Seigler, and E. C. Gage, Heat-assisted magnetic recording by a near-field transducer with efficient optical energy transfer, *Nat. Photonics* 3(4), 220 (2009)
251. B. C. Stipe, T. C. Strand, C. C. Poon, H. Balamane, T. D. Boone, J. A. Katine, J. L. Li, V. Rawat, H. Nemoto, A. Hirotsume, O. Hellwig, R. Ruiz, E. Dobisz, D. S. Kercher, N. Robertson, T. R. Albrecht, and B. D. Terris, Magnetic recording at 1.5 Pb m^{-2} using an integrated plasmonic antenna, *Nat. Photonics* 4(7), 484 (2010)
252. R. Vincent, H. Marinchio, J. J. Saenz, and R. Carminati, Local control of the excitation of surface plasmon polaritons by near-field magneto-optical Kerr effect, *Phys. Rev. B* 90(24), 241412 (2014)
253. P. S. Keatley, A. Aziz, M. Ali, B. J. Hickey, M. G. Blamire, and R. J. Hicken, Optical characterization of nonlocal spin transfer torque acting on a single nanomagnet, *Phys. Rev. B* 89(9), 094421 (2014)
254. P. Biagioni, J. S. Huang, L. Duo, M. Finazzi, and B. Hecht, Cross resonant optical antenna, *Phys. Rev. Lett.* 102(25), 256801 (2009)
255. Z. Zhang, A. Weber-Bargioni, S. W. Wu, S. Dhuey, S. Cabrini, and P. J. Schuck, Manipulating nanoscale light fields with the asymmetric Bowtie nano-colorsorter, *Nano Lett.* 9(12), 4505 (2009)
256. A. McLeod, A. Weber-Bargioni, Z. Zhang, S. Dhuey, B. Harteneck, J. B. Neaton, S. Cabrini, and P. J. Schuck, Non-perturbative visualization of nanoscale plasmonic field distributions via photon localization microscopy, *Phys. Rev. Lett.* 106(3), 037402 (2011)
257. P. Biagioni, M. Savoini, J. S. Huang, L. Duo, M. Finazzi, and B. Hecht, Near-field polarization shaping by a near-resonant plasmonic cross antenna, *Phys. Rev. B* 80(15), 153409 (2009)
258. D. Lin and J. S. Huang, Slant-gap plasmonic nanoantennas for optical chirality engineering and circular dichroism enhancement, *Opt. Express* 22(7), 7434 (2014)
259. Y. Tang and A. E. Cohen, Enhanced enantioselectivity in excitation of chiral molecules by superchiral light, *Science* 332(6027), 333 (2011)
260. E. Hendry, T. Carpy, J. Johnston, M. Popland, R. V. Mikhaylovskiy, A. J. Lapthorn, S. M. Kelly, L. D. Barron, N. Gadegaard, and M. Kadodwala, Ultrasensitive detection and characterization of biomolecules using superchiral fields, *Nat. Nanotechnol.* 5(11), 783 (2010)
261. B. le Feber, N. Rotenberg, and L. Kuipers, Nanophotonic control of circular dipole emission, *Nat. Commun.* 6, 6695 (2015)
262. I. Söllner, S. Mahmoodian, S. L. Hansen, L. Midolo, A. Javadi, G. Kiršanskė, T. Pregnolato, H. El-Ella, E. H. Lee, J. D. Song, S. Stobbe, and P. Lodahl, Deterministic photon-emitter coupling in chiral photonic circuits, *Nat. Nanotechnol.* 10(9), 775 (2015)
263. J. Rudge, H. Xu, J. Kolthammer, Y. K. Hong, and B. C. Choi, Sub-nanosecond time-resolved near-field scanning magneto-optical microscope, *Rev. Sci. Instrum.* 86(2), 023703 (2015)